Flow and freeze-out predictions in a combined macro/micro transport approach

S.A. Bass *
Department of Physics
Duke University
Durham, NC, 27708-0305, USA

A. Dumitru †
Department of Physics
Columbia University
538W 120th Street, New York, NY 10027, USA

We predict flow and freeze-out observables in the framework of a combined macroscopic/microscopic transport approach, utilizing a boost-invariant one-fluid hydrodynamics model for the initial, dense reaction stage and a non-equilibrium microscopic hadronic transport model for the later, dilute phase of the reaction.

I. THE MODEL:

In our model, we use boost-invariant hydrodynamics to describe a first order phase transition from a QGP to a hadronic fluid, and combine it with a non-equilibrium microscopic transport calculation for the later, purely hadronic stages of the reaction. With this ansatz we are able to self-consistently calculate the freeze-out of the system: no decoupling hypersurface is imposed by hand, but the space-time points are rather determined by an interplay between the (local) expansion scalar ∂u [5,4] (where u is the collective flow four-velocity), the relevant elementary cross sections, and the equation of state (EoS), which actually changes dynamically as more and more hadron species decouple.

Let us first briefly describe the hydrodynamical model employed here: For a more detailed discussion we refer to refs. [3,6,7]. For simplicity, boost-invariant longitudinal flow [1] is assumed. For ultrarelativistic collisions, this should be a reasonable first approximation in the central rapidity region. Cylindrically symmetric transverse expansion is superimposed. For $T > T_C = 160$ MeV the well-known MIT bag model equation of state [8] is used, assuming for simplicity an ideal gas of quarks, anti-quarks (with masses $m_u = m_d = 0$, $m_s = 150$ MeV), and gluons. For $T < T_C$ an ideal hadron gas is employed that includes the complete hadronic spectrum up to a mass of 2 GeV. At $T = T_C, (\mu_B = \mu_S = 0)$ we require that both pressures are equal, which fixes the bag constant to $B = 380$ MeV/fm^3. By construction the EoS exhibits a first order phase transition (which is also expected in QCD for the quark-hadron phase transition in the case of three quark flavors).

The model reproduces the measured p_T- and m_T-spectra of hadrons at the SPS, when assuming that hydrodynamic flow sets in on the proper time hyperbola $\tau_i = 1$ fm/c [3,6]. This is a value conventionally assumed in the literature, cf. e.g. [1]. Due to the higher parton density at midrapidity, thermalization may be reached earlier at RHIC [9]. As in refs. [3,6], we assume here $\tau_i = R_T/10 = 0.6$ fm. The effects of variations of τ_i and T_C are discussed in detail in [7]. Moreover, we use the initial average energy and baryon densities $\overline{\epsilon}(\tau_i) = 20$ GeV/fm^3 and $\overline{\rho}(\tau_i) = 2.3\rho_0$, which lead to $dN_B/dy = 25$ and $\overline{s}/\overline{\rho}_B = 205$ (a bar symbols an average over the transverse plane). The initial energy and net baryon densities are assumed to be distributed in the transverse plane according to a so-called "wounded nucleon" distribution $\propto \frac{3}{2}\sqrt{1 - r_T^2/R_T^2}$, with transverse radius $R_T = 6$ fm. For this set of parameters, the initial transverse energy at midrapidity is $\mathrm{d}E_T/\mathrm{d}y = 1.3$ TeV. Due to the work performed by the isentropic expansion, it decreases to 716 GeV on the hadronization hypersurface. The microscopic treatment of the hadronic dynamics following hadronization (see below) yields $\mathrm{d}E_T/\mathrm{d}y = 714$ GeV at kinetic freeze-out. Thus, the late hadronic evolution at RHIC energy is not isentropic.

After specifying the initial conditions and the EoS, we determine numerically the hydrodynamical solution between the $\tau = \tau_i$ hyperbola and the hadronization hypersurface, where we apply the Cooper-Frye formula [10] to obtain the hadron spectra. However, in contrast to the usual procedure we do not integrate over the hypersurface, because we further on also need the *space-time* distribution of hadrons emerging from the mixed phase, not only their momentum-space distributions [6]. The ensemble of hadrons thus generated is then used as initial condition for the non-equilibrium microscopic transport model Ultra-relativistic Quantum Molecular Dynamics (UrQMD) [11].

---

*e-mail address: bass@phy.duke.edu
†e-mail address: dumitru@mail-cunuke.phys.columbia.edu

The UrQMD model contains hadronic (and string) degrees of freedom – all hadronic states can be produced in string decays, s-channel collisions or resonance decays. Tabulated and parameterized experimental cross sections are used when available. Resonance absorption, decays and scattering are handled via the principle of detailed balance. The UrQMD model has been extensively tested in the SIS, AGS and SPS energy domain and provides a robust description of hadronic heavy-ion physics phenomenology. An extensive description of the model, as well as comparisons with various available data can be found in [11].

During the mixed phase the system is either described *locally* within the hydrodynamical framework (as long as a non-zero fraction of the fluid in the cell consists of quark and gluons) or within the microscopic transport (in the case of pure hadronic matter). Therefore there exists a time interval during the reaction in which both models are applied in parallel, even though they never refer locally to the same space-time volume.

II. PREDICTIONS:

Figure 1 shows the time evolution of on-shell hadron multiplicities. The dark grey shaded area indicates the duration of the QGP phase whereas the light grey shaded area depicts the mixed phase (both averaged over r_T; only hadrons that have already "escaped" from the mixed phase are shown). Hadronic resonances are formed and are populated for a long time ($\approx$ 20fm/c). When the mixed phase ceases to exist, the hadron yields have not yet saturated (even if resonance decays are taken into account). This is due to inelastic hadron-hadron collisions. In particular the yield of anti-protons drops strongly – more than 60% of the baryon-anti-baryon annihilations occur after the phase-coexistence is over. The yields of all stable hadrons at midrapidity can be extracted from the figure for the limit of $\tau \to \infty$. They saturate at approximately 25 fm/c – only then may the system be viewed as chemically frozen-out. Since resonance decays have not been included into our estimate of the saturation time, this number may be viewed as an upper estimate of the chemical freeze-out time.

The freeze-out characteristics of the nucleons are significantly modified due to the hadronic interaction phase. The average transverse freeze-out radius doubles at SPS and RHIC and increases by a factor of 2.5 at LHC (see also table I). The respective average freeze-out times increase by similar factors (see table II). E.g., at RHIC the average freeze-out time for protons changes from 11.3 to 25.8 fm/c due to hadronic rescattering.

As the meson multiplicity in the system at RHIC is fifty times larger than the baryon multiplicity, baryons propagate through a relativistic meson gas, acting as probes of this highly excited meson medium. Thus, we use the proton and hyperon freeze-out values listed in table II for a first rough estimate of the duration of the hadronic phase via $\Delta\tau_{had} = \langle\tau_{fr}^{\rm Hydro+UrQMD}\rangle - \langle\tau_{fr}^{\rm Hydro+had.decays}\rangle$. At the SPS $\Delta\tau_{had}$ is found to be $\approx$ 13.5 fm/c, very similar to the value at RHIC ($\approx$ 15 fm/c) and at the LHC we obtain $\Delta\tau_{had} \approx 23$ fm/c. The transverse spatial extent of the hadronic phase can be estimated in a similar way, using table I and defining the *thickness* Δr_{had} of the hadronic phase as: $\Delta r_{had} = \langle r_{t,fr}^{\rm Hydro+UrQMD}\rangle - \langle r_{t,fr}^{\rm Hydro+had.decays}\rangle$. Here we find values of $\approx$ 4.4 fm at the SPS, $\approx$ 5.8 fm at RHIC and $\approx$ 13.3 fm at the LHC.

The Hydro+UrQMD model predicts a space-time freeze-out picture which is very different from that usually employed in the hydrodynamical model, e.g. in refs. [3,5,4,12,13]: Here [7], freeze-out is found to occur in a *four-dimensional* region within the forward light-cone [14] rather than on a three-dimensional "hypersurface" [10]. Similar results have also been obtained within other microscopic transport models [15] when the initial state was not a quark-gluon plasma. This finding seems to be a generic feature of such models: the elementary binary hadron-hadron interactions smear out the sharp signals to be expected from simple hydro. This predicted additional fourth dimension of the freeze-out domain could affect the HBT parameters considerably.

Figure 2 shows the estimated freeze-out volume $V^* = \pi\langle r_{T,fr}\rangle^2\langle\tau_{fr}\rangle$ as a function of the pion rapidity density $\mathrm{d}N_\pi/\mathrm{d}y$ for four different bins in transverse momentum. For all p_T-bins V^* exhibits a nearly linear increase with $\mathrm{d}N_\pi/\mathrm{d}y$. Thus, the freeze-out density of the pions remains virtually constant over a large range of multiplicities (or energies). We will see in the next section that this is due to the fact that the chemical freeze-out of pions occurs rather shortly after hadronization of the QGP, at all energies studied here. Since the local density of pions on the hadronization hypersurface is similar in all cases (because the temperature is almost the same), the density at chemical freeze-out is, too.

We also observe that low-p_T pions are basically emitted from the entire volume, while at higher p_T the pions seem only to be emitted from an outer *shell*, the radius of the hollow core increasing with p_T. The inset of figure 2 shows the dependence of the non-emitting core-volume V_0 on the transverse momentum of the pions. V_0 has been calculated by a linear fit of V^* to $\mathrm{d}N_\pi/\mathrm{d}y$: $V^* = V_0 + c\,(\mathrm{d}N_\pi/\mathrm{d}y)$. The increase of V_0 with p_T is a manifestation of the collective flow effect; high-p_T pions can not be emitted from the center, $r_T \sim 0$, since the collective velocity field vanishes there.

Fig. 3 compares the m_T-spectra on the hadronization hypersurface including strong resonance decays (open symbols), with those at freeze-out (full symbols). One observes that the transverse flow of p's and Λ's increases during the hadronic stage, since those spectra flatten. On the other hand, the spectra of Ω's and of Ξ's with $m_T > 1.6$ GeV are practically unaffected by the hadronic stage and closely resemble those on the phase boundary. This is due to the fact that the scattering rates of Ξ and Ω in a pion-rich hadron gas are significantly smaller than those of N's and Λ's [16,6,17]. As shown in [6,7], on average the baryons which finally emerge as Ξ's and Ω's suffer far less interactions than the final-state p's and Λ's. Thus, within the model presented here, these particles are basically emitted *directly from the phase boundary* with very little further rescattering in the hadronic stage. The hadron gas emerging from the hadronization of the QGP (in these high-energy reactions) is almost "transparent" for the multiple strange baryons. On the other hand, p's and Λ's on average suffer several collisions with other hadrons before they freeze-out. This behavior holds generally true for all three studied energy domains, at the SPS, RHIC and LHC.

These findings manifest themselves most strikingly in the mass-dependence of the inverse slopes of the m_T spectra. A simple isentropic hydrodynamical expansion leads to broader m_T spectra of heavier states, i.e. $\langle p_T\rangle$ or the inverse slope T^* increase with mass [18]. This observation agrees with the inverse slopes of π, K, and p measured for central collisions of Pb nuclei at a CM-energy of $17A$ GeV [19]. However, it has also been found that the Ξ and Ω baryons do not follow this general trend [20,21].

Fig. 4 depicts the inverse slopes T^* obtained from our model by a fit of $\mathrm{d}^3N_i/\mathrm{d}^2m_T\mathrm{d}y$ to $\exp(-m_T/T^*)$ in the range $m_T - m_i < 1$ GeV. The statistical error of this fit is $\sim 10\%$. Open symbols denote the SPS calculation and data, whereas full symbols show the RHIC prediction. The lines show a purely hydrodynamical calculation [3,6] with a freeze-out temperature of $T_{fo} = 130$ MeV for SPS (dotted line) and RHIC (full line), respectively. The trend of the SPS data (open circles), namely the "softer" spectra of Ξ's and Ω's as compared to a linear $T^*(m)$ relation, is reproduced reasonably well. As already mentioned, this is not the case for "pure" hydrodynamics with kinetic freeze-out on a common hypersurface (e.g. the $T = 130$ MeV isotherm), where the stiffness of the spectra increases monotonically with mass, cf. Fig. 4 and also refs. [4,22]. Resonance decays are not included in the hydrodynamic spectra on the $T = 130$ MeV isotherm.

When going from SPS to RHIC energy, the model discussed here generally yields only a slight increase of the inverse slopes, although the specific entropy is larger by a factor of 4-5 ! The reason for this behavior is the first-order phase transition that softens the transverse expansion considerably [23]. For our set of initial conditions, the *average* collective transverse flow velocity (at mid-rapidity) on the hadronization hypersurface increases only from ≈ 0.3 (for Pb+Pb at SPS) to ≈ 0.35 (for Au+Au at RHIC) [3]. (However, there are high-v_T tails on the hadronization hypersurface which get more pronounced at RHIC than at SPS.) As can be seen from the present calculation, this is not counterbalanced by increased rescattering in the purely hadronic stage – compare to the inverse slopes obtained from "pure" hydrodynamics with freeze-out on the $T = 130$ MeV isotherm!

The transverse flow at LHC beam energy is so strong that the m_T-spectra can not be fitted any more by an exponential distribution. We have therefore refrained to extract the slopes for the LHC calculation. Instead, in figure 5 we show the mean transverse momenta of the different hadron species as a function of their mass. As in figure 3 we compare the $\langle p_T\rangle$ on the hadronization hypersurface including strong resonance decays (open symbols), with that at freeze-out (full symbols). Hadronic rescattering leads to a transfer of transverse energy/momentum from pions to heavier hadrons (the pions actually suffer a reduction of $\langle p_T\rangle$ in the hadronic phase) [24]. This phenomenon has also been termed the *pion-wind* [4,25], pushing heavier hadrons to higher p_T. Nucleons gain most transverse momentum, while the Ω^- remains nearly unchanged due to its small interaction cross section in the meson dominated hadronic medium, as discussed earlier in this section. Those hadrons are the best "messengers" of the early pre-hadronization evolution. Furthermore, one clearly observes the rather moderate increase of $\langle p_T\rangle$ from SPS to RHIC energy, as discussed already in Fig. 4. This $\langle p_t\rangle$-plateau occurs due to the release of latent heat in the first-oder phase transition [26]. In contrast, in our model the collective dynamics at the much higher CERN-LHC energy is dominated by the stiff QGP and the average transverse momenta increase appreciably.

---

[1] J.D. Bjorken, Phys. Rev. **D27** (1983) 140.
K. Kajantie and L. McLerran, Nucl. Phys. **B214** (1983) 261.

[2] D.H. Rischke and M. Gyulassy, Nucl. Phys. **A597** (1996) 701, and **A608** (1996) 479.
S. Bernard, D.H. Rischke, J.A. Maruhn, W. Greiner, Nucl. Phys. **A625** (1997) 473.

[3] A. Dumitru and D.H. Rischke, Phys. Rev. **C59** (1999) 354.

[4] C.M. Hung and E. Shuryak, Phys. Rev. **C57** (1998) 1891.

[5] I. Mishustin and L. Satarov, Sov. J. Nucl. Phys. **37** (1983) 532.

[6] A. Dumitru, S.A. Bass, M. Bleicher, H. Stöcker, and W. Greiner, Phys. Lett. **B460**, 411 (1999).

[7] S.A. Bass and A. Dumitru, Phys. Rev. **C** in print, [nucl-th/0001033].
[8] A. Chodos, R.L. Jaffe, K. Johnson, C.B. Thorn and V.F. Weisskopf, Phys. Rev. **D9** (1974) 3471.
[9] K. Geiger, Phys. Rev. **D46** (1992) 4986.
[10] F. Cooper and G. Frye, Phys. Rev. **D10** (1974) 186.
[11] S. A. Bass, M. Belkacem, M. Bleicher, M. Brandstetter, L. Bravina, C. Ernst, L. Gerland, M. Hofmann, S. Hofmann, J. Konopka, G. Mao, L. Neise, S. Soff, C. Spieles, H. Weber, L. A. Winckelmann, H. Stöcker, W. Greiner, C. Hartnack, J. Aichelin and N. Amelin, Progr. Part. Nucl. Physics Vol. **41**, 225 (1998), nucl-th/9803035
M. Bleicher, E. Zabrodin, C. Spieles, S.A. Bass, C. Ernst, S. Soff, L. Bravina, M. Belkacem, H. Weber, H. Stöcker and W. Greiner, J. Phys. **G25**, 1859 (1999) The UrQMD source code is available via the URL:
`http://www.th.physik.uni-frankfurt.de/~urqmd`
[12] J. Cleymans, K. Redlich, and D.K. Srivastava, Phys. Rev. **C55**, 1431 (1997).
[13] Y. Sinyukov, Z. Phys. **C43**, 401 (1989);
L.P. Csernai, Z.I. Lazar, and D. Molnar, Heavy Ion Physics **5**, 467 (1997).
[14] F. Grassi, Y. Hama, and T. Kodama, Z. Phys. **C73**, 153 (1996);
F. Grassi, Y. Hama, T. Kodama and O. Socolowski, Heavy Ion Phys. **5**, 417 (1997);
F. Grassi and O.J. Socolowski, Phys. Rev. Lett. **80**, 1170 (1998).
[15] L.V. Bravina, I.N. Mishustin, N.S. Amelin, J.P. Bondorf, and L.P. Csernai, Phys. Lett. **B354**, 196 (1995);
H. Sorge, Phys. Lett. **B373**, 16 (1996).
[16] H. van Hecke, H. Sorge, and N. Xu, Phys. Rev. Lett. **58**, 5764 (1998).
[17] M. Bleicher, C. Spieles, C. Ernst, L. Gerland, S. Soff, H. Stöcker, W. Greiner, and S.A. Bass, Phys. Lett. **B447**, 227 (1999).
[18] P.J. Siemens and J.O. Rasmussen, Phys. Rev. Lett. **42**, 880 (1979);
H. Stöcker, A.A. Ogloblin, and W. Greiner, Z. Phys. **A303**, 259 (1981).
[19] I.G. Bearden et al., (NA44 Collab.), Phys. Rev. Lett. **78**, 2080 (1997).
[20] E. Andersen et al. (WA97 Collaboration), Phys. Lett. **B433**, 209 (1998);
E. Andersen et al. (WA97 Collaboration), J. Phys. **G25**, 181 (1999).
[21] P.G. Jones and the NA49 collaboration, Nucl. Phys. **A610**, 188c (1996);
C. Bormann et al., (NA49 collaboration), J. Phys. **G23**, 1817 (1997);
H. Appelshäuser et al., (NA49 collaboration), Phys. Lett. **B444**, 523 (1998).
[22] T. Csörgö and B. Lörstad, Phys. Rev. **C54**, 1390 (1996);
B. Kämpfer, O.P. Pavlenko, A. Peshier, M. Hentschel, and G. Soff, J. Phys. **G23**, 2001 (1997).
[23] C.M. Hung and E. Shuryak, Phys. Rev. Lett. **75**, 4003 (1995);
T.S. Biro, nucl-th/9911004.
[24] S. Pratt and J. Murray, Phys. Rev. **C57**, 1907 (1998).
[25] Y. Pang et al., http://rhic.phys.columbia.edu/oscar;
M. Bleicher, S.A. Bass, L.V. Bravina, W. Greiner, H. Stöcker, N. Xu and E. Zabrodin, hep-ph/9911420.
[26] M. Kataja, P.V. Ruuskanen, L. McLerran and H. von Gersdorff, Phys. Rev. **D34**, 2755 (1986).

$\langle r_t \rangle$ (fm)	SPS			RHIC			LHC		
species	d.p.b.	h.r.	h.t.	d.p.b.	h.r.	h.t.	d.p.b.	h.r.	h.t.
π	6.9	8.4	1.5	7.8	9.5	1.7	12.3	16.8	4.5
K	6.2	8.4	2.2	7.1	10.2	3.1	11.4	18.1	6.7
p	4.7	9.1	4.4	5.4	11.3	5.9	8.7	22.2	13.5
Y	5.1	9.5	4.4	5.8	11.6	5.8	9.6	22.7	13.1
Ξ	8.3	12.1	3.8	9.4	14.2	4.8	8.7	22.1	13.4
Ω^-	4.4	6.3	1.9	4.7	7.3	2.6	7.3	13.9	6.6

TABLE I. Mean transverse freeze-out radii $\langle r_T \rangle$ for different hadron species at SPS, RHIC and LHC. *d.p.b* denotes the transverse freeze-out radii of the hydrodynamical calculation up to hadronization, including subsequent hadronic decays, but no hadronic reinteractions, *h.r.* denotes the full Hydro+UrQMD calculation, including hadronic rescattering and *h.t.* stands for an estimate of the *thickness* Δr_{had} of the hadronic phase: $\Delta r_{had} = \langle r_{T,fr}^{\mathrm{Hydro+UrQMD}} \rangle - \langle r_{T,fr}^{\mathrm{Hydro+had.decays}} \rangle$.

$\langle\tau\rangle$ (fm/c)	SPS			RHIC			LHC		
species	d.p.b.	h.r.	h.d.	d.p.b.	h.r.	h.d.	d.p.b.	h.r.	h.d.
π	16.1	21.8	5.7	17.2	23.1	5.9	21.2	31.2	10.0
K	13.5	20.2	6.7	14.7	22.7	8.0	18.8	31.9	13.1
p	10.6	23.7	13.1	11.3	25.8	14.5	14.6	37.2	22.6
Y	11.3	25.0	13.7	12.0	27.4	15.4	15.6	39.0	23.4
Ξ	19.9	31.0	11.1	20.4	32.2	11.8	14.1	36.2	22.1
Ω^-	8.6	16.2	7.6	9.3	17.3	8.0	12.3	25.1	12.8

TABLE II. Mean freeze-out times for different hadron species at SPS, RHIC and LHC. *d.p.b* denotes the freeze-out times of the hydrodynamical calculation up to hadronization, including subsequent hadronic decays, but no hadronic reinteractions, *h.r.* denotes the full Hydro+UrQMD calculation, including hadronic rescattering and *h.d.* stands for an estimate of the *duration* of the hadronic reinteraction phase, $\Delta\tau_{had} = \langle\tau_{fr}^{\mathrm{Hydro+UrQMD}}\rangle - \langle\tau_{fr}^{\mathrm{Hydro+had.decays}}\rangle$.

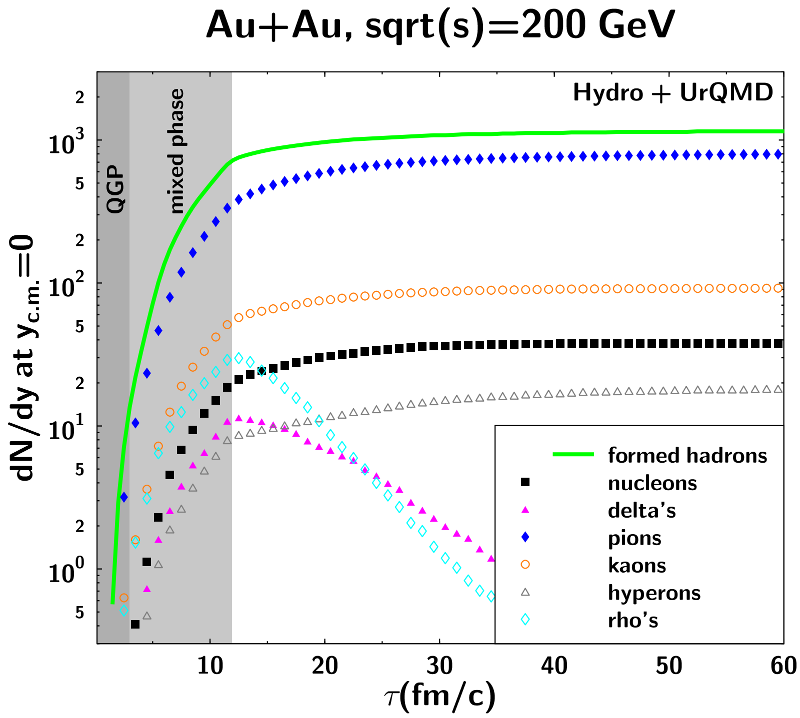

FIG. 1. Time evolution of on-shell hadron multiplicities (integrated over r_T). The dark grey shaded area shows the duration of the QGP phase whereas the light grey shaded area depicts the coexistance phase.

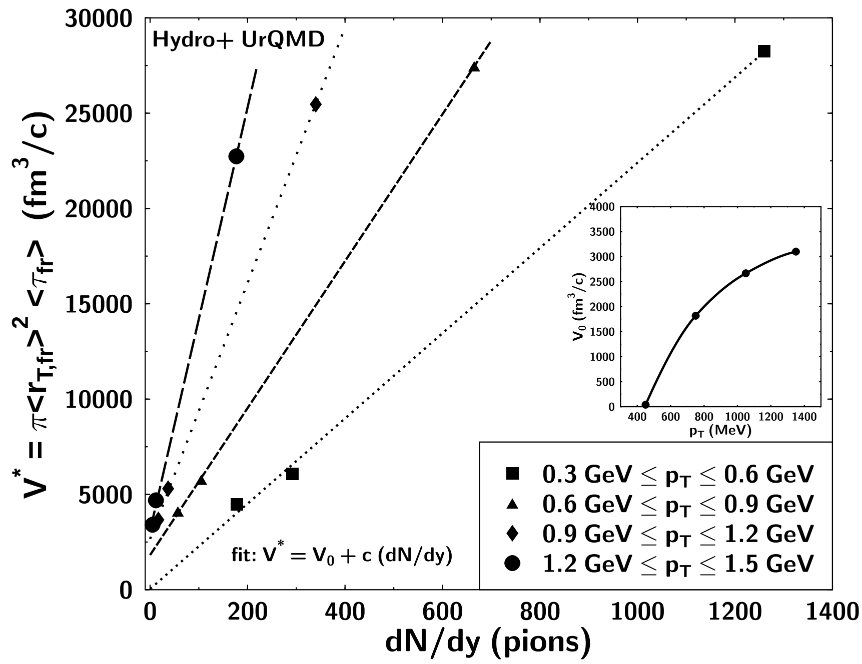

FIG. 2. Estimated freeze-out volume of pions as a function of the pion rapidity density for four different bins in transverse momentum. High p_T-pions are only emitted from an outer *shell*, the radius of which increases with p_T. The inset shows the volume of the "hollow core" as a function of p_T.

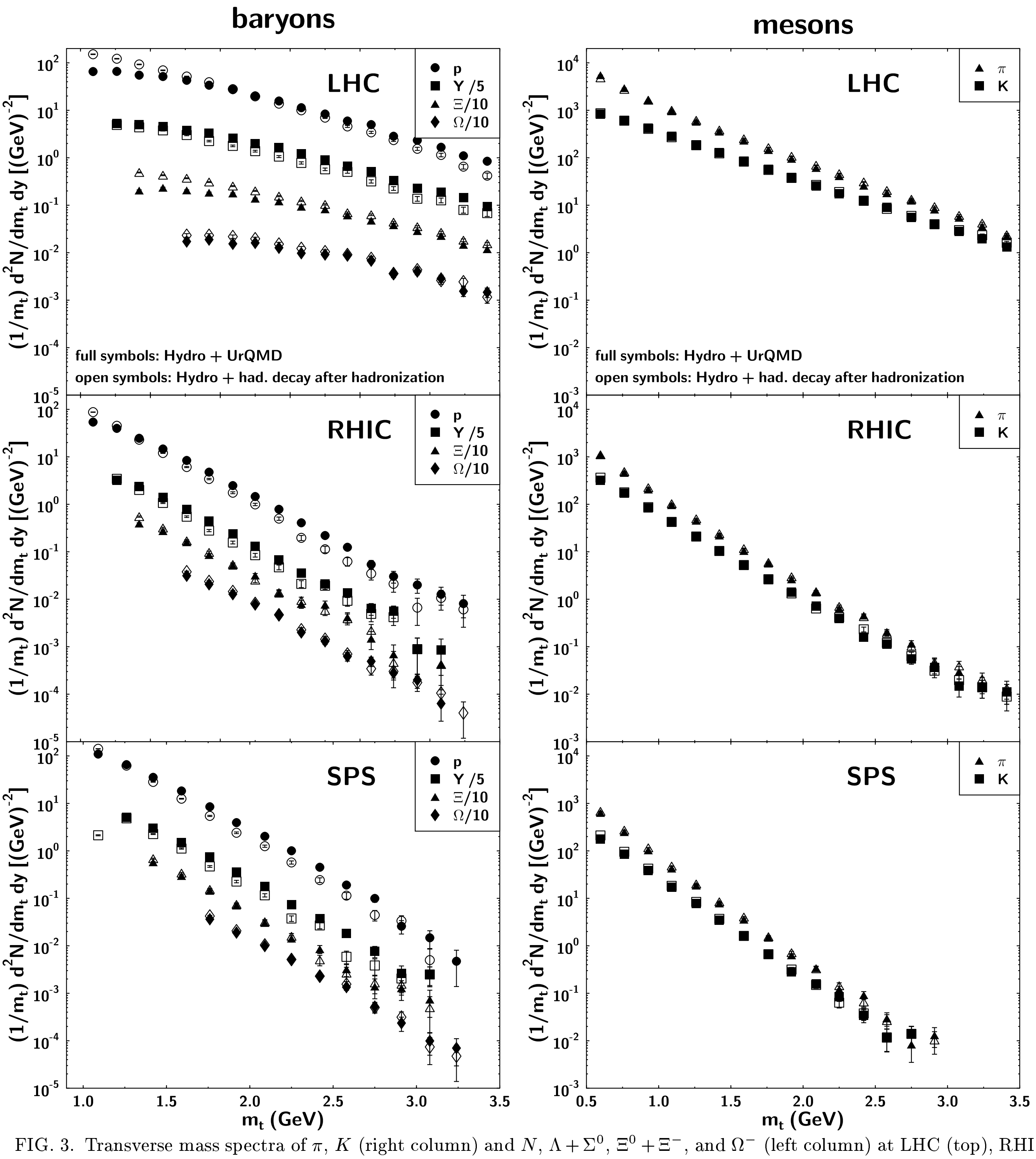

FIG. 3. Transverse mass spectra of π, K (right column) and N, $\Lambda+\Sigma^0$, $\Xi^0+\Xi^-$, and Ω^- (left column) at LHC (top), RHIC (middle) and SPS (bottom). The open symbols denote the spectra on the hadronization hypersurface whereas the full symbols show the calculation at freeze-out after hadronic rescattering.

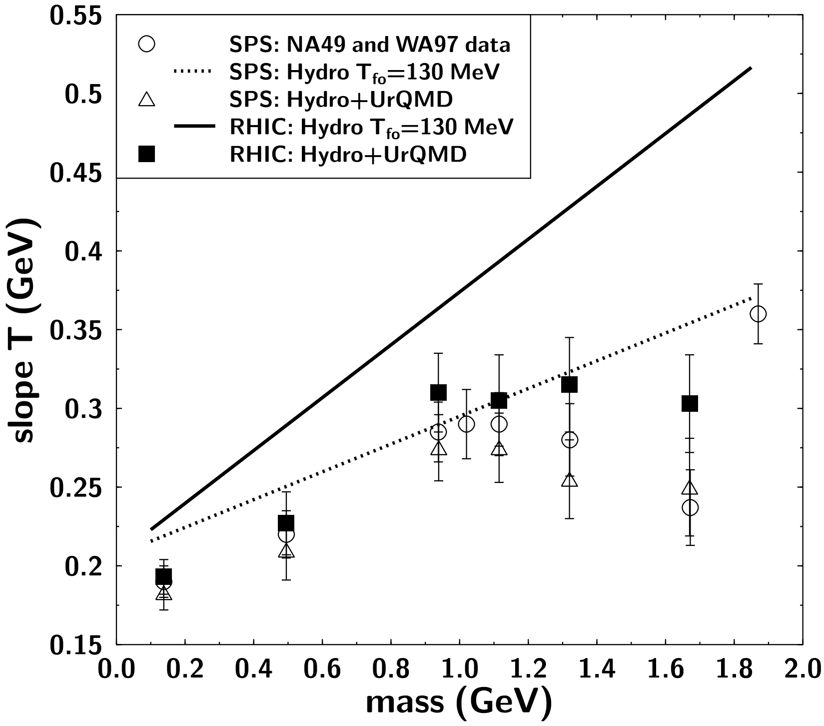

FIG. 4. Inverse slopes of the m_T-spectra of π, K, p, $\Lambda + \Sigma^0$, $\Xi^0 + \Xi^-$, and Ω^- at $y_{c.m.} = 0$, $m_T - m_i < 1$ GeV.

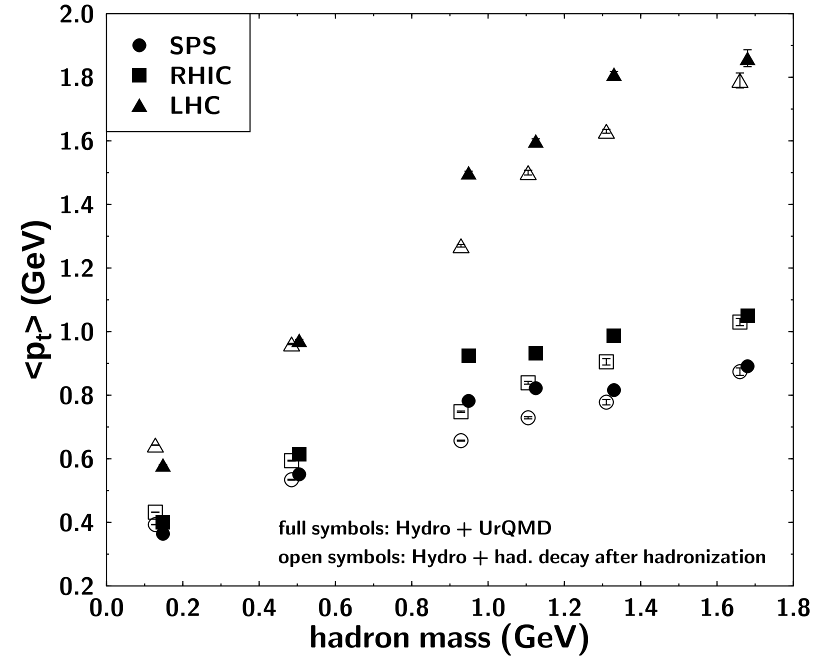

FIG. 5. Average transverse momentum $\langle p_T \rangle$ vs. mass for π, K, p, Y, Ξ and Ω. The open symbols denote the spectra on the hadronization hypersurface (including strong resonance decays), the full symbols show the value at freeze-out (after hadronic rescattering). For clarity, the symbols have been shifted by ± 10 MeV.